Journal of Sound and Vibration 330 (2011) 337–355

Contents lists available at ScienceDirect

Journal of Sound and Vibration

journal homepage: www.elsevier.com/locate/jsvi

Analysis of nonlinear oscillators using Volterra series in the frequency domain

L.M. Li, S.A. Billings*

Department of Automatic Control and Systems Engineering, University of Sheffield, Sheffield S1 3JD, UK

ARTICLE INFO

Article history:
Received 29 January 2010
Accepted 8 August 2010
Handling Editor: L.N. Virgin
Available online 9 September 2010

ABSTRACT

The Volterra series representation is a direct generalisation of the linear convolution integral and has been widely applied in the analysis and design of nonlinear systems, both in the time and the frequency domain. The Volterra series is associated with the so-called weakly nonlinear systems, but even within the framework of weak nonlinearity there is a convergence limit for the existence of a valid Volterra series representation for a given nonlinear differential equation. Barrett (1965) [1] proposed a time domain criterion to prove that the Volterra series converges within a given region for a class of nonlinear systems with cubic stiffness nonlinearity. In this paper this time-domain criterion is extended to the frequency domain to accommodate the analysis of nonlinear oscillators subject to harmonic excitation. A common and severe nonlinear phenomenon called jump, a behavior associated with the Duffing oscillator and the multi-valued properties of the response solution, is investigated using the new frequency domain criterion of establishing the upper limits of the nonlinear oscillators, to predict the onset point of the jump, and the Volterra time and frequency domain analysis of this phenomenon are carried out based on graphical and numerical techniques.

1. Introduction

Nonlinear Volterra theory was initially proposed by Volterra [2]. The theory quickly received a great deal of attention in the field of electrical engineering, mechanical engineering, and later in the biological field, as a powerful approach for modelling nonlinear system behaviors. From the late 1950s, there has been a continuous effort in the application of Volterra series to nonlinear systems theory. Summaries of major contributions in the application of Volterra series modelling for the representation, analysis and design of nonlinear systems can be found in [3–6].

Based on the Volterra series representation, generalised frequency response functions (GFRFs) have proved to be powerful in the analysis and design of nonlinear systems in the frequency domain [7]. However, this analysis can only be directly applied to so-called weakly nonlinear systems, which usually represent a small subset of the rich characteristics of nonlinear dynamics. It is therefore desirable to have a simple criterion establishing the boundary between weak nonlinearity and severe nonlinearity in the frequency domain.

In this paper a new method is proposed to find the convergence region for a class of nonlinear oscillators with cubic stiffness nonlinearity subject to harmonic excitation. A typical example of this kind of oscillator is the Duffing oscillator. The Duffing oscillator has been extensively applied to represent many practical systems and is often used as a benchmark

* Corresponding author. Tel.: +44 114 2225232.
E-mail addresses: L.Li@Sheffield.ac.uk (L.M. Li), S.Billings@sheffield.ac.uk (S.A. Billings).

0022-460X/$ - see front matter © 2010 Elsevier Ltd. All rights reserved.
doi:10.1016/j.jsv.2010.08.016

example for nonlinear oscillator analysis in electrical and mechanical engineering [8]. A severe nonlinear phenomenon, referred to as jump, induced by the multi-valued solution due to the cubic nonlinearity, is very commonly seen in the Duffing oscillator. Jump phenomenon is seemly a time domain phenomenon, but in fact it is closely associated with the Volterra frequency domain representation, therefore the new method of establishing the upper limit of Duffing oscillators are applied to explain the mechanism behind this phenomenon and to provide a prediction of the onset point for this behavior change. In addition, time and frequency domain modelling of this phenomenon are performed.

This paper is organised as follows. In Section 2 the Volterra/frequency modelling for single-input–single-output nonlinear systems is reviewed. In Section 3, the extension of the Barrett's time domain method [1] to the frequency domain to accommodate harmonic excitation is presented. In Section 4, numerical examples are used to demonstrate the new approach, along with the comparison with previous approaches. In Section 5, the application of the new approach in the identification of jump phenomenon is studied. In Section 6, the Volterra modelling of Duffing systems that exhibit jump phenomenon is discussed. Finally in Section 7, conclusions are given.

2. Volterra modelling in the time and frequency domain

Volterra series modelling has been widely studied for the representation, analysis and design of nonlinear systems. The Volterra model is a direct generalisation of the linear convolution integral, therefore providing an intuitive representation in a simple and easy to apply way. For a SISO nonlinear system, where $u(t)$ and $y(t)$ are the input and output, respectively, the Volterra series can be expressed as

$$y(t)=\sum_{n=1}^{\infty} y_n(t) \tag{1}$$

and $y_n(t)$ is the 'nth order output' of the system

$$y_n(t)=\int_{-\infty}^{\infty}\cdots\int_{-\infty}^{\infty} h_n(\tau_1,\ldots,\tau_n)\prod_{i=1}^{n} u(t-\tau_i)\,\mathrm{d}\tau_i,\quad n>0 \tag{2}$$

where $h_n(\tau_1,\ldots,\tau_n)$ is called the 'nth-order kernel' or 'nth-order impulse response function'. If $n=1$, this reduces to the familiar linear convolution integral.

In practice only the first few kernels are used on the assumption that the contribution of the higher order kernels falls off rapidly. Systems that can be adequately represented by a Volterra series with just a few terms are called a weakly or mildly nonlinear system.

A valid Volterra series representation means valid generalised frequency response functions (GFRFs). The GFRFs are obtained by taking the multidimensional Fourier transform of $h_n(\cdot)$:

$$H_n(\omega_1,\ldots,\omega_n)=\int_{-\infty}^{\infty}\cdots\int_{-\infty}^{\infty} h_n(\tau_1,\ldots,\tau_n)\exp(-j(\omega_1\tau_1+\cdots+\omega_n\tau_n))\,\mathrm{d}\tau_1\cdots\mathrm{d}\tau_n \tag{3}$$

The generalised frequency response functions represent an inherent and invariant property of the underlying system, and have proved to be an important analysis and design tool for characterizing nonlinear phenomena. In practice, the GFRFs can be estimated using non-parametric or parametric methods. The parametric method involves mapping a nonlinear differential equation [9] or mapping a nonlinear difference equation [10] into the frequency domain using the probing method.

3. Derivation of convergence region in the frequency domain

Barrett was one of the first people to carry out a systematic study of the application of Volterra series to the analysis of nonlinear differential equations and nonlinear feedback systems [11]. A new time domain approach for finding the convergence region of the derived Volterra series representation under arbitrary inputs was later proposed by Barrett [1]. In this paper this time domain approach is extended to the frequency domain to accommodate the case of nonlinear oscillations subject to harmonic excitations.

Considering the following system with cubic stiffness nonlinearity

$$L\left(\frac{\mathrm{d}}{\mathrm{d}t}\right)y(t)+k_3y^3(t)=u(t) \tag{4}$$

where k_3 is a small constant and $L(q)=q^p+a_1q^{p-1}+\cdots+a_p$ with the assumption that $L(q)=0$ has roots with negative real parts. The initial conditions are set equal to zero.

Initially, the time domain convergence analysis proposed by Barrett [1] will be briefly illustrated.

The nonlinear system (4) has a Volterra series representation which includes the 1st and 3rd order kernels

$$y(t)=\int_{-\infty}^{\infty} h_1(t-\tau)u(\tau)\,\mathrm{d}\tau-k_3\int\int\int_{-\infty}^{\infty} h_3(t-\tau_1,t-\tau_2,t-\tau_3)u(\tau_1)u(\tau_2)u(\tau_3)\,\mathrm{d}\tau_1\,\mathrm{d}\tau_2\,\mathrm{d}\tau_3 \tag{5}$$

where

$$h_3(t-\tau_1,t-\tau_2,t-\tau_3)=\int_{-\infty}^{\infty}h_1(t-\tau)h_1(t-\tau_1)h_1(t-\tau_2)h_1(t-\tau_3)\,\mathrm{d}\tau \tag{6}$$

Denoting

$$\|u\|=\sup_{-\infty<t<\infty}|u(t)|,\quad \Theta=\int_0^{\infty}|h(t)|\,\mathrm{d}t$$

For a convergent Volterra expression, each of the terms in (5) needs to be bounded. For the first term,

$$\left|\int_{-\infty}^{\infty}h(t-\tau)u(\tau)\,\mathrm{d}\tau\right|\le\int_{-\infty}^{\infty}|h(t-\tau)||u(\tau)|\,\mathrm{d}\tau\le\Theta\|u\| \tag{7}$$

Similarly for the second term, by using (6),

$$\begin{aligned}\left|\int\int\int_{-\infty}^{\infty}h_3(t-\tau_1,t-\tau_2,t-\tau_3)u(\tau_1)u(\tau_2)u(\tau_3)\,\mathrm{d}\tau_1\,\mathrm{d}\tau_2\,\mathrm{d}\tau_3\right|&\le\int\int\int_{-\infty}^{\infty}|h_3(t_1,t_2,t_3)|\,\mathrm{d}t_1\,\mathrm{d}t_2\,\mathrm{d}t_3\|u\|^3\\&=\int\int\int_{-\infty}^{\infty}\left|\int_{-\infty}^{\infty}h_1(t')h_1(t_1-t')h_1(t_2-t')h_1(t_3-t')\,\mathrm{d}t'\,\mathrm{d}t_1\,\mathrm{d}t_2\,\mathrm{d}t_3\|u\|^3\right|\\&\le\int\int\int\int_{-\infty}^{\infty}|h_1(t')||h_1(t_1-t')||h_1(t_2-t')||h_1(t_3-t')|\,\mathrm{d}t'\,\mathrm{d}t_1\,\mathrm{d}t_2\,\mathrm{d}t_3\|u\|^3\\&\le\int_{-\infty}^{\infty}|h_1(t')|\,\mathrm{d}t'\int_{-\infty}^{\infty}|h_1(t_1-t')|\,\mathrm{d}t_1\int_{-\infty}^{\infty}|h_1(t_2-t')|\,\mathrm{d}t_2\int_{-\infty}^{\infty}|h_1(t_3-t')|\,\mathrm{d}t_3\|u\|^3\\&=\left(\int_{-\infty}^{\infty}|h_1(t)|\,\mathrm{d}t\right)^4\|u\|^3=\Theta^4\|u\|^3\end{aligned} \tag{8}$$

Therefore, each term of the Volterra series representation in (5) does not exceed, in absolute magnitude, the corresponding term of a certain power series

$$Y=\Phi(U)=\Theta U+|k_3|\Theta^4U^3 \tag{9}$$

provided that $\|u\|<U$.

In fact the solution of (9) is a series solution of the equation

$$Y-|k_3|\Theta Y^3=\Theta U \tag{10}$$

by the method of successive approximation.

Barrett [1] proved that the Volterra series (5) is convergent if $\|u\|<U_1$ where

$$U_1=2/[\sqrt{|k_3|}(3\Theta)^{3/2}] \tag{11}$$

Nonlinear systems described by (4) represent a large number of single-degree-of-freedom physical systems with nonlinear stiffness and widely exist in circuits, aircraft, marine engineering, etc. Most of the dynamics of these nonlinear systems, such as hysteresis, limit cycles, bifurcations and chaos, were built in the framework of nonlinear oscillation and vibration subject to harmonic excitations. It is therefore desirable to extend the purely time domain criterion (11) into the frequency domain by probing the system using harmonic excitation.

Assume the excitation is in the harmonic form

$$u(t)=Ae^{j\omega t}\ \text{with}\ A>0$$

The first term in (5) is bounded by

$$\begin{aligned}\left|\int_{-\infty}^{\infty}h(t-\tau)u(\tau)\,\mathrm{d}\tau\right|&=A\left|\int_{-\infty}^{\infty}h(\tau)e^{j\omega(t-\tau)}\,\mathrm{d}\tau\right|=A\left|\int_{-\infty}^{\infty}h(\tau)e^{j\omega(t-\tau)}\,\mathrm{d}\tau\right|\\&=A\left|e^{j\omega t}\int_{-\infty}^{\infty}h(\tau)e^{-j\omega\tau}\,\mathrm{d}\tau\right|=A|e^{j\omega t}H_1(\omega)|\le A|e^{j\omega t}||H_1(\omega)|\le A|H_1(\omega)|\end{aligned} \tag{12}$$

using the definition $H_1(\omega)=\int_{-\infty}^{\infty}h(\tau)\exp(-j\omega\tau)\,\mathrm{d}\tau$

Similarly the second term in (5) is bounded by

$$\left|\int\int\int_{-\infty}^{\infty}h_3(t-\tau_1,t-\tau_2,t-\tau_3)u(\tau_1)u(\tau_2)u(\tau_3)\,\mathrm{d}\tau_1\,\mathrm{d}\tau_2\,\mathrm{d}\tau_3\right|\le A^3|H_1(\omega)|^4 \tag{13}$$

Hence the response of the Volterra series representation (5) will not exceed, in absolute magnitude,

$$\hat{Y}=A|H_1(\omega)|+|k_3|A^3|H_1(\omega)|^4 \tag{14}$$

with $\hat{Y}$ the successive approximation of

$$\hat{Y}-|k_3||H_1(\omega)|\hat{Y}^3=A|H_1(\omega)| \tag{15}$$

The maximum amplitude $\tilde{A}$ of excitation allowed to have a convergent Volterra series at different excitation frequency ω can be obtained by solving $dA/d\hat{Y}=0$ in (15) to give

$$\tilde{A}(\omega)=2/[\sqrt{|k_3|}(3|H_1(\omega)|)^{3/2}] \tag{16}$$

Note that

$$|H_1(\omega)|=\left|\int_0^\infty h(\tau)e^{j\omega(t-\tau)}\,d\tau\right|\le\int_0^\infty |h(\tau)||e^{j\omega(t-\tau)}|\,d\tau\le\int_0^\infty |h(\tau)|\,d\tau=\Theta \tag{17}$$

Therefore, the following result holds between the time domain criterion (11) and the frequency domain criterion (16):

$$U_1\le\min_{0<\omega<\infty}(\tilde{A}(\omega)) \tag{18}$$

(18) reflects the fact that Barrett's time domain criterion, which deals with arbitrary excitation and with harmonic excitation as a special case, represents the worst case and is therefore a conservative result.

4. Numerical illustrations and discussions

By setting p=2 with $u(t)$ in sinusoidal format, (4) reduces to

$$\ddot{y}+a_1\dot{y}+a_2y+k_3y^3=A\cos(\omega t) \tag{19}$$

which is the well-known Duffing's oscillator, introduced by Duffing in 1918 to describe a mechanical problem under periodic forces and later also widely used to represent electronic circuits, etc. It is one of the most common examples in the study of nonlinear oscillations. Typically in a mechanical format Duffing's oscillator is described as

$$m\ddot{y}+c\dot{y}+k_1y+k_3y^3=A\cos(\omega t) \tag{20}$$

where m is the mass, c is the damping, k_1 is proportional to the stiffness of the spring, and k_3 is the cubic stiffness. $k_3>0$ models a hardening nonlinearity, and $k_3<0$ models a softening nonlinearity. The upper limit of excitation level which allows a valid Volterra series representation under both hardening and softening nonlinearity situations will be discussed next. A valid Volterra series representation means valid GFRFs from which the steady-state estimation of the response can be generated. Because the Duffing equation (20) contains a cubic nonlinear term y^3, all even orders of GFRFs are zero and make no contribution to the system response. The steady-state response using GFRFs can be found for example in [12].

4.1. Hardening nonlinearity

A number of criteria to find the upper limits of the magnitude of harmonic excitation in Duffing's oscillator with $k_3>0$ have been proposed [13–15]. Ref. [15] pointed out that the criterion proposed in [14] based on a ratio test procedure was essentially the same as [13] with different computational approaches. Therefore, only the results in [13,15] are presented here for discussion.

Criterion in [13] is defined as

$$\tilde{A}_T(\omega)<\left[\tfrac{2}{3}(k_3|H_1(\omega)|^3\right]^{-1/2} \tag{21}$$

which is similar to the extended Barrett's result (16) but differs in magnitude, and criterion [14] is defined as

$$\tilde{A}_P(\omega)<\frac{1}{|H_1(\omega)|\sqrt{\lambda k_3}} \tag{22}$$

where

$$\lambda=\max_{k=1,\ldots,\infty}(|H_1((2k-1)\omega|) \tag{23}$$

The coefficients of the Duffing oscillator used in the numerical study are

$$m=1,\quad c=1.5,\quad k_1=0.5,\quad k_3=0.1 \tag{24}$$

The frequency domain criteria by (16), (21) and (22) are shown in Fig. 1.

Barrett's time domain result by (11), in this example, is exactly the minimum value from the new frequency domain criterion (16), that is

$$U_1=\min_{0<\omega<\infty}(\tilde{A}(\omega))=0.43 \tag{25}$$

which occurs at ω=0.

It can be seen from Fig. 1 that in the low frequency range the results of the different criterion are not significantly different, but as the frequency increases the system can endure higher and higher levels of excitation with a valid Volterra series solution, and the difference between different criteria becomes more and more significant. For example, at ω=2.5 rad/s, the result by criterion (23) is $\tilde{A}_T(\omega)|_{\omega=2.5}=46.44$. Exciting the Duffing system (26) at level A=45 which is

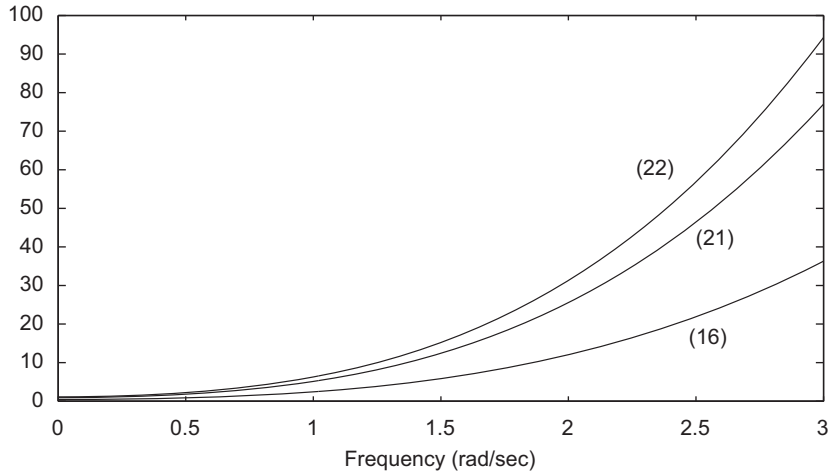

Fig. 1. Frequency domain criterion by (16), (21) and (22).

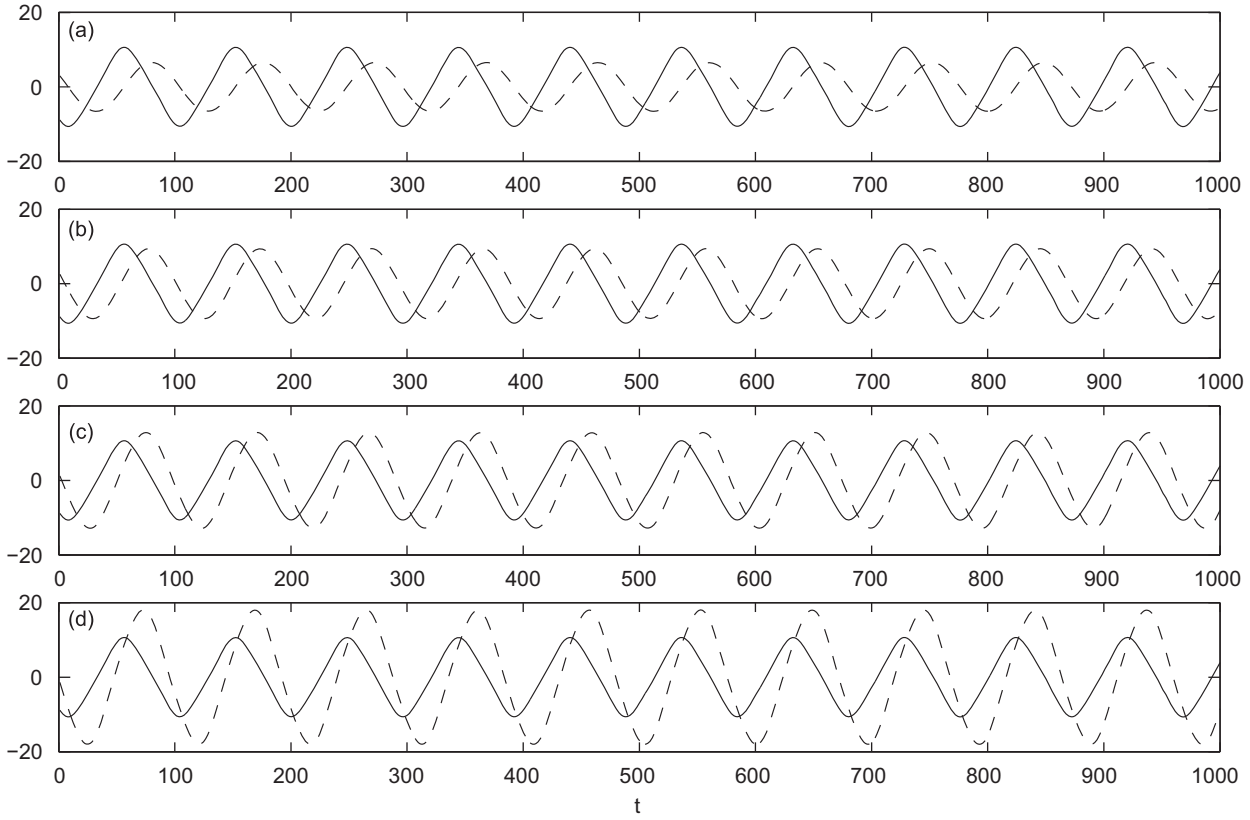

Fig. 2. (a) First order output response, (b) up to the 3rd order response, (c) up to the 5th order response, and (d) up to the 7th order response. Dashed—synthesized output by GFRFs; solid—simulated original output from (24).

within the region set out by $\tilde{A}_T(\omega)$, the resulting real response and the synthesized response up to 7th order GFRFs are compared in Fig. 2.

A clearer numerical measure of the closeness of fit between the synthesized response and the real response can be obtained by using the normalised root mean square error defined as

$$NMSE = \sqrt{\frac{\sum (y_{\mathrm{syn}}(t) - y_{\mathrm{real}}(t))^2}{\sum (y_{\mathrm{real}}(t) - y_{\mathrm{mean}}(t))^2}} \tag{26}$$

where $y_{syn}(t)$ is the synthesized response and $y_{mean}(t)$ is the mean value of the real data set $y(t)$. Table 1 shows the NMSE in different approximation orders.

The results in Fig. 2 and Table 1 suggest that the Volterra representation at this excitation level is not convergent.

In addition, the power spectrum of the real response is illustrated in Fig. 3, showing an overwhelmingly dominant first harmonic presence, compared with other higher order harmonics. Whereas in Fig. 2(a) there is a large bias in the first order harmonic estimation, in terms of both amplitude and phase. It can be argued that even theoretically there is a convergent Volterra series representation around this level of excitation, this convergence can only be achieved at the high cost of employing extremely high order GFRFs in order to compensate the bias in the first order harmonic. This makes the Volterra series representation or the application of GFRFs using the original system description (24) uneconomic in terms of computational burden and expression, and therefore less practical.

Table 1
Comparison of NMSE between the real response and synthesized response.

	1st order synthesis	Up to 3rd order synthesis	Up to 5th order synthesis	Up to 7th order synthesis
NMSE	1.1646	1.1944	1.2586	1.4729

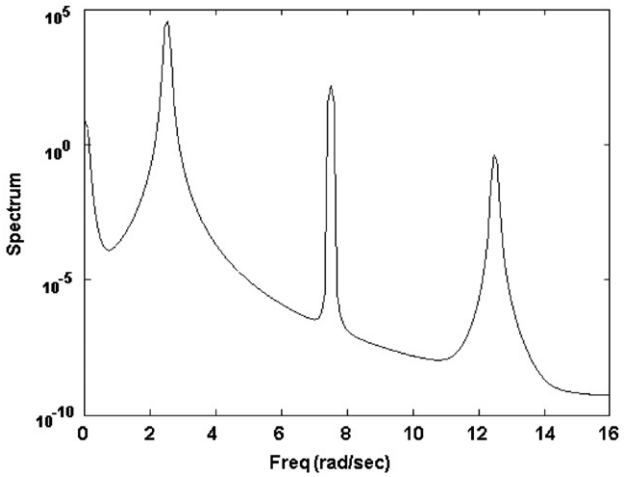

Fig. 3. Power spectrum of the real response from system (24) at A=45.

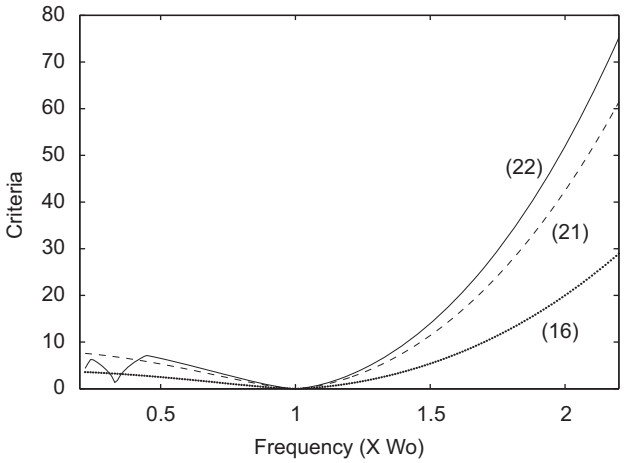

Fig. 4. The criteria by (16)—dot, (21)—dashed and (22)—solid.

Consider another example. By denoting $\omega_0=\sqrt{k_1/m}$, $\mu=c/(2\omega_0)$, $\varepsilon=k_3/k_1$, $A_0=(1/m)A$, (20) can be transferred to the other commonly used form

$$\ddot{y}+2\mu\omega_0\dot{y}+\omega_0^2y+\varepsilon\omega_0^2y^3=A_0\cos(\omega t) \tag{27}$$

which has been studied in [15].

A comparison of the criteria is shown in Fig. 4 using (16), (21) and (22) respectively. Again in the low frequency range, there are small differences between all the criteria (16), (21) and (22) for locating the upper limits of the Volterra series representation under harmonic excitation. In particular, the criterion (22) in [15] can provide a more accurate estimation of the excitation limit at the $\frac{1}{3}\omega_0$ sub-resonant frequency. While as the frequency increases to greater than the natural resonance frequency ω_0, as the system experiences more complicated dynamics, the differences between the criteria become more and more significant. The frequency dynamics of the underlying system can be more easily studied by a diagram called the response spectrum map (RSM), which was proposed by Billings and Boaghe [16] as a frequency domain alternative to the traditional bifurcation diagram. One such RSM is shown in Fig. 5 at $\omega=2.1\omega_0$, with $A_1=24.23$, $A_2=51.42$ and $A_3=62.97$ in the figure corresponding to the criteria (16), (21) and (22), respectively. The line H1 represents the first order harmonics ω (fundamental frequency) and the line H3 is the third-order harmonics 3ω and so on. It is very clear

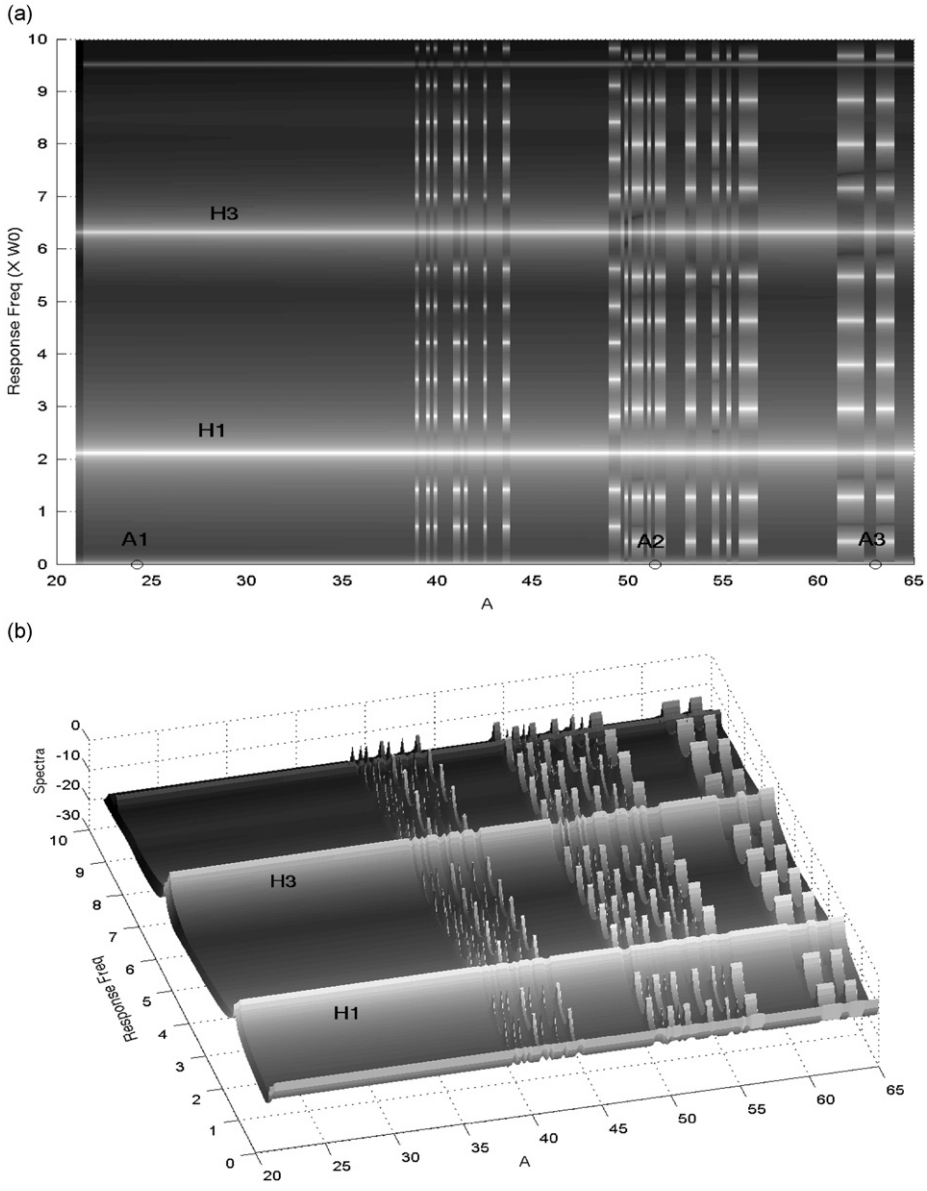

Fig. 5. Response spectrum map of Duffing oscillator (27) at $\omega=2.1\omega_0$: (a) 2D view and (b) 3D view.

from Fig. 5 that for $38 < A < 50$, the system has $\frac{1}{3}$subharmonics in the response at most frequencies, and for $50 < A < 65$ the system experiences $\frac{1}{5}$ subharmonics. It is well known that the Volterra series cannot be used to directly model the system that exhibits subharmonics, this means that in this case, the values A_2 and A_3, which are well into the subharmonic zone, are overestimated. It can also be easily examined that the real convergent upper limit for this case is around A=21, which is close to the new result A_1=24.23 by (16).

4.2. Softening nonlinearity

The other frequency domain criteria mentioned in section 4.1 excludes the situation when the cubic stiffness is less than zero. Generally speaking when $k_3 < 0$, the Duffing oscillator has a more restricted convergence region than that for $k_3 > 0$.

The coefficients of the Duffing oscillator used in the softening nonlinearity case are

$$m = 1, \quad c = 1.5, \quad k_1 = 0.5, \quad k_3 = -0.1 \tag{28}$$

The frequency dynamics of the underlying system can be illustrated by the response spectrum map (RSM) in Fig. 6. It can be seen from Fig. 6 that, before the system becomes unstable at A=3.99, it experiences a very brief window in which

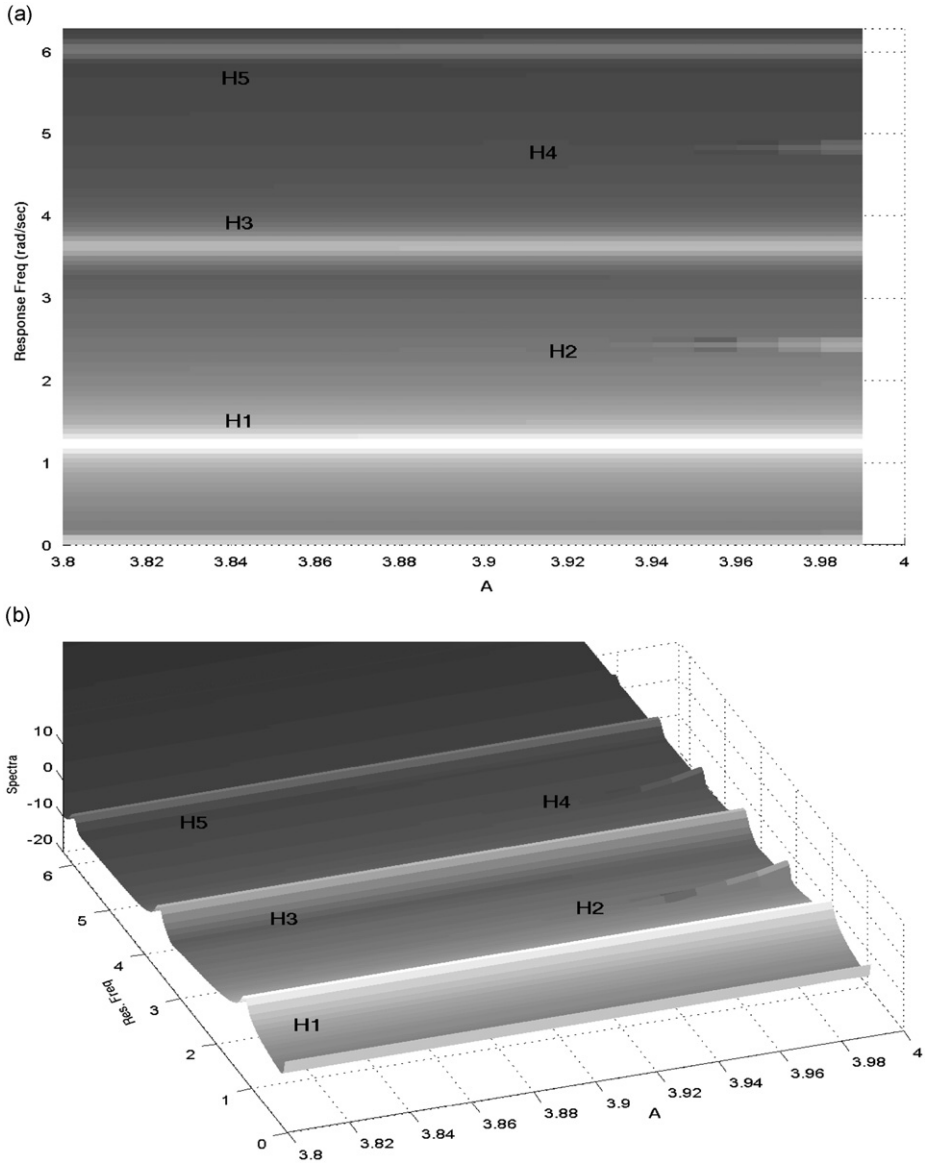

Fig. 6. Response spectrum map for system (28) at ω=1.2: (a) 2D view and (b) 3D view.

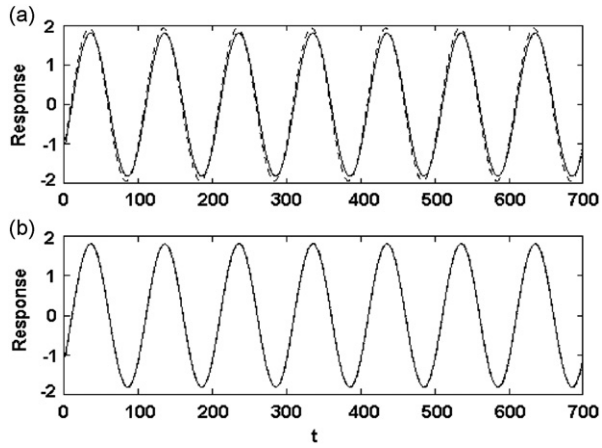

Fig. 7. (a) First order output response, (b) up to the third-order response. Dashed—synthesized output by GFRFs; solid—simulated original output from (28).

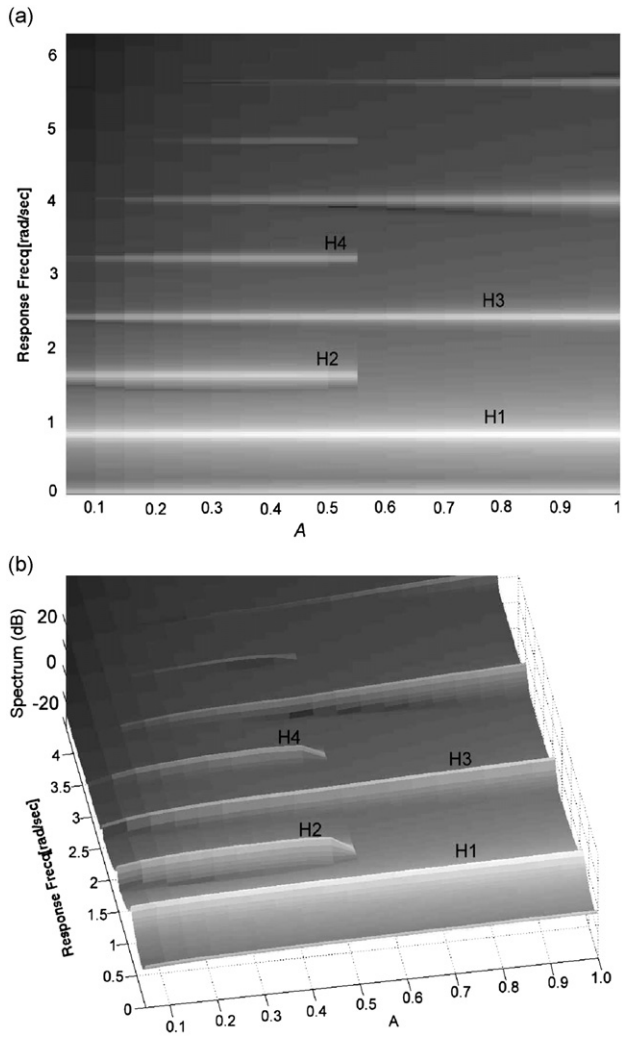

Fig. 8. RSM for Duffing–Holmes oscillator (30): (a) 2D view and (b) 3D view.

the response contains, in addition to the odd order harmonics H1, H3, H5, etc., also even order harmonics components H2 and H4 (very weak though) over $3.93 < A < 3.99$. Theoretically this means that the existence of a Volterra series representation for this amplitude range is ruled out. For $A < 3.93$ the response contains standard odd order harmonics, that is, ω, 3ω and 5ω, etc. Therefore A=3.93 can be regarded as the decision point between the existence and non-existence of a valid Volterra series representation for the Duffing oscillator (28) at ω=1.2. This decision value is close to the result given by the new criterion (16) at $\tilde{A}(\omega)|_{\omega=1.2} = 3.52$. It is interesting to analyze the frequency domain synthesis of the response using GFRFs, as shown in Fig. 7, at the decision point $\tilde{A} = 3.93$.

It is clear from Fig. 7 that a fast convergence can be achieved by using only the first and 3rd orders of Volterra kernels. This suggests that a quick convergence of Volterra series representation as assumed from the derivations of (16) has practical grounds.

4.3. The case when $L(q)$ has unstable roots

The criterion (16) is based on the assumption that the linear part of the nonlinear oscillator is stable, that is, the roots of $L(q)$=0 in (4) have negative real parts.

This restriction was not explicitly imposed by the previous criteria (21) and (22), etc. The necessity of this restriction can be made evident in the following simulation. Fig. 8 shows the RSM of a Duffing–Holmes oscillator with the parameters

$$m = 1, \quad c = 1.5, \quad k_1 = -0.2, \quad k_3 = 1 \tag{29}$$

and excitation frequency $\omega = 0.8\,\mathrm{rad/s}$.

It is clear from Fig. 8 that for the lower amplitude range $A < 0.57$ there are 0, ω, 2ω, 3ω, 4ω, ... harmonics, which immediately rules out the existence of a valid Volterra series representation. For $A > 0.57$ valid Volterra series representations can be derived from (29) until the excitation level A reaches around 1.6. Therefore this essentially means that the original system (29) can only possibly produce a convergent Volterra series representation over a narrow band of external excitation levels, rather than within a radius of convergence, making any of the previous mentioned criteria inapplicable. Further work is needed to solve this class of problem.

5. Identification of jump phenomenon

5.1. Preliminaries

Despite the seemly simple form of Duffing's oscillator (20), it is extremely rich in dynamic behavior and exhibits many complex solutions. Almost every nonlinear phenomenon can be found in Duffing's equation therefore it has often been used as a benchmark example in many studies. The bifurcation diagram in Fig. 9 shows some typical dynamics of a Duffing oscillator with the parameters in (20) as

$$m = 1, \quad c = 0.4, \quad k_1 = 1, \quad k_3 = 4 \tag{30}$$

at ω=2.5 rad/s.

It can be seen from Fig. 9 that the Duffing oscillator experiences dramatic dynamic behaviors during the course of excitation amplitude changes. Among them, there is a period-doubling (1/2 subharmonics) for $43 < A < 50.5$, a further period-doubling (1/4 subharmonics) for $50.5 < A < 52$, leading to chaos regime for $52 < A < 55$. Subharmonics and chaos

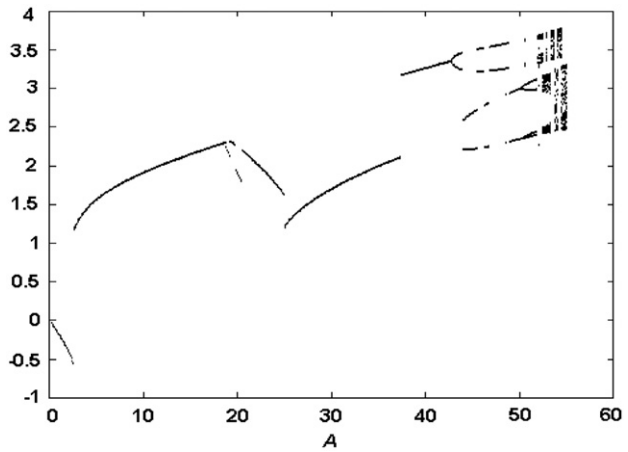

Fig. 9. Bifurcation diagram for system (30).

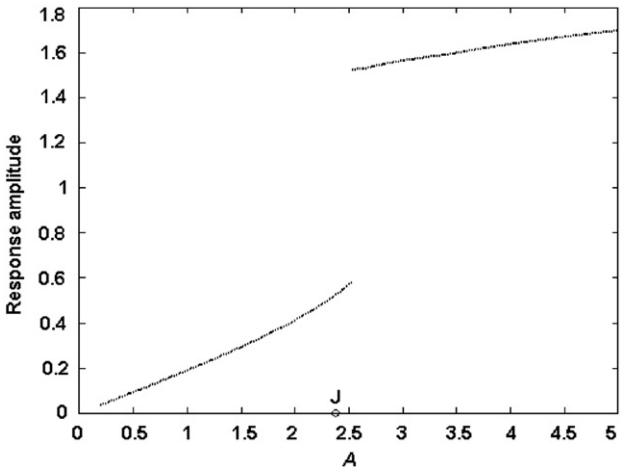

Fig. 10. Response amplitude jump of system (30).

are two of the most common phenomena occurring in nonlinear oscillators and have attracted constant interest and study over the past decades [17–24].

Another commonly occurring nonlinear phenomenon is the shock jump, shown in Fig. 9 over the excitation level $2 < A < 3$. As Pain [25] pointed out the amplitude of the response is not single valued for a given frequency where shock jumps in response amplitude may occur.

A zoomed view is shown in Fig. 10 for the amplitude of response against the excitation level around the jump, which is the main subject of this study. Unlike subharmonics and chaos, this kind of severe nonlinear problem has received little attention to date. In the following sections, the prediction, analysis and modelling of the jump phenomenon using Volterra series in the frequency domain are introduced for the first time.

5.2. Analysis of jump phenomenon in the frequency domain

As noted in subsection 5.1 of section 5, the Duffing oscillator (30) can represent very complex dynamic behaviors. For such a driven nonlinear oscillator, closed-form analytical solutions are not available therefore approximation schemes are used in quantitative investigations. One of the approximation methods that have been widely adopted is the harmonic balance method. This involves re-arranging the external excitation in (20) as

$$u = P\sin(\omega t) + Q\cos(\omega t) \;\text{ with } A = \sqrt{P^2 + Q^2} \tag{31}$$

and expressing the response as

$$y = C\sin(\omega t) \tag{32}$$

Substituting (31) and (32) into (20), together with the use of $\sin^3(t) = \frac{3}{4}\sin(t) - \frac{1}{4}\sin(3t)$ yields

$$\tfrac{3}{4}k_3H^3\sin(\omega t) - mH\omega^2\sin(\omega t) + cH\sin(\omega t) + k_1H\omega c\cos(t) = P\sin(t) + Q\cos(t) \tag{33}$$

where the term containing $\sin(3\omega t)$ has been neglected.

Equating coefficients of the same harmonic terms in (33) and using $A = \sqrt{P^2 + Q^2}$ gives [7]

$$\left[\tfrac{3}{4}k_3C^3 + (k_1 - m\omega^2)C\right]^2 + c^2\omega^2C^2 = A^2 \tag{34}$$

Because of the cubic nonlinearity $k_3 \neq 0$, the response will be multi-valued, shown in Fig. 11.

Comparing Figs. 11 and 10 reveals that the estimated harmonic balance solutions provide a good approximation of the real solution in terms of both value and trend. Inspection of Fig. 11 reveals that, when increasing the amplitude A to around 1.4 until 2.8, two stable solutions will co-exist (the shadow range in Fig. 11). When some certain conditions are met, the solution will jump from one to the other. However, (34) cannot provide any indication on why and when this type of severe dynamic change will happen.

It is easy to verify that for the Solution 1 range, the original system (30) can provide a valid Volterra series/GFRF representation for the underlying system. This also indicates that, considering the analytic nature of Volterra series representation, the original system (30) will no longer be valid in the Volterra/GFRFs domain from the start of Solution 2, or the response jumping point. This implies that the jumping point is the upper limit of the Volterra series representation for this type of nonlinear system.

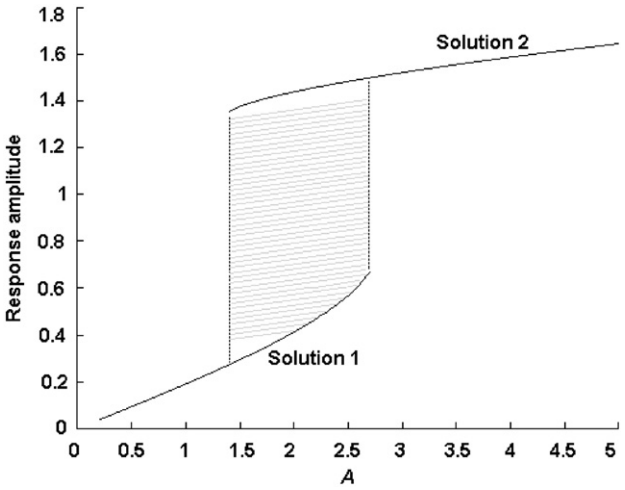

Fig. 11. Harmonic balance solutions from (34) for system (30).

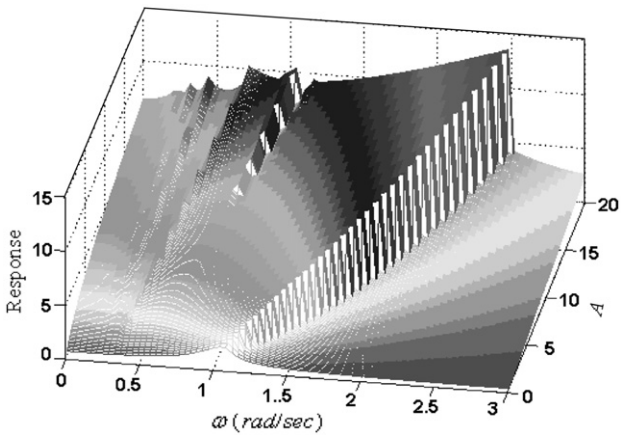

Fig. 12. Response map of the Duffing oscillator (35) for both varying excitation amplitude and frequency.

The result of the new criterion (16) for system (30) at ω=2.5 rad/s is shown in Fig. 10 as point '*J*', which is a good estimation of the real jump point. This is not exceptional but, as the following example shows, a general rule for this kind of problem.

Consider a Duffing oscillator with the parameters

$$m=1, \quad c=0.2, \quad k_1=1 \text{ and } k_3=0.05 \tag{35}$$

Fig. 12 gives a clear overall picture of when and where the jump occurs along both varying excitation amplitude and frequency axes.

The jump cliff starts from ω=1 rad/s and A=1. The frequency point and the magnitude of the jump increase monotonically, as the amplitude of the excitation increases, showing a clear pattern. The rule that governs the pattern is indeed the criterion (16), as shown in Fig. 13, in which the real jump line is the 2-D overhead view from Fig. 12. It can be seen that the result by criterion (16) predicts very accurately the real jumping points.

For comparison, the recent frequency domain criteria (21) and (22) are also displayed in Fig. 13.

Note that here the jumping line is the absolute splitting line dividing the validity and in-validity of the Volterra series representation for the original system (35). Clearly both (21) and (22) are significantly overestimated in the jumping case.

Take a cross section of Fig. 12 at ω=2 rad/s, shown in Fig. 14.

In this example the jump occurs at A=9.09, which agrees very well with the criterion (7) at $\tilde{A}(\omega)|_{\omega=2}=9.06$. The new criterion (16) was proposed based on the assumption that the system can be well described by the first few Volterra kernels and for which the higher order kernels fall off rapidly. This can be verified by exploring the response in terms of Volterra/GFRF representation right before and after the jump, as illustrated in Fig. 15.

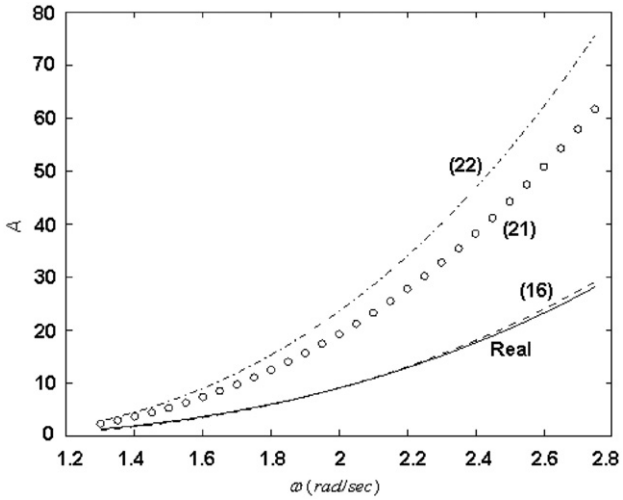

Fig. 13. Comparison of real jump line with different Volterra criteria. Real—solid; criterion (16)—dashed; criterion (21)—circled, criterion (22)—dash dotted.

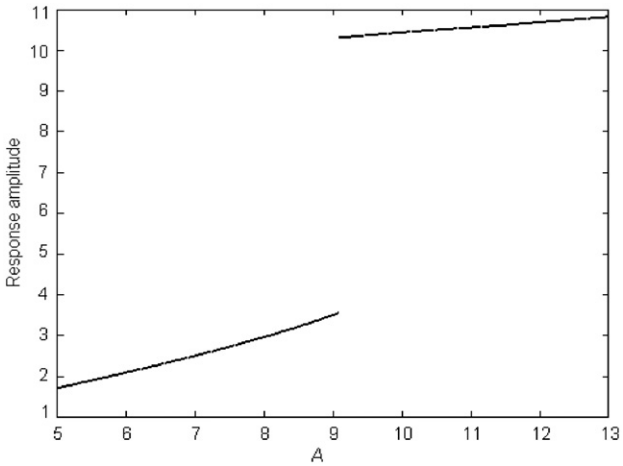

Fig. 14. Response amplitude jump for system (35) at ω=2 rad/s.

So far we can conclude that fast convergence or representation efficiency is likely to be the mechanism behind the triggering of jumping. When the amplitude of excitation increases to the upper limit of a fast convergence low order Volterra series representation as (16) suggested, the response will be forced to jump to the other stable solution, making the original Duffing system no longer valid in the Volterra/frequency domain. This dramatic dynamic change has its appearance in the time domain, but actually has solid roots in the frequency domain. It is of therefore of interest to make a frequency domain investigation using response spectrum map (RSM) [16].

Fig. 16 shows that the harmonic components of response of system (30) remain the same, both before and after the jump. The difference lies in the strength of the fundamental and higher order harmonics (cf. Fig. 16). This suggests that, although a global Volterra series representation is not possible from the description of the original system (35) for the range after the jump, a local Volterra series representation is still possible by means of discrete time parametric modelling.

First, the discrete time domain Volterra expression is introduced as

$$y(k) = \sum_{n=1}^{\infty} y_n(k) \tag{36}$$

where

$$y_n(k) = \sum_{-\infty}^{\infty} \cdots \sum_{-\infty}^{\infty} h_n(\tau_1, \ldots, \tau_n) \prod_{i=1}^{n} u(k-\tau_i), \quad n > 0, \quad k \in Z$$

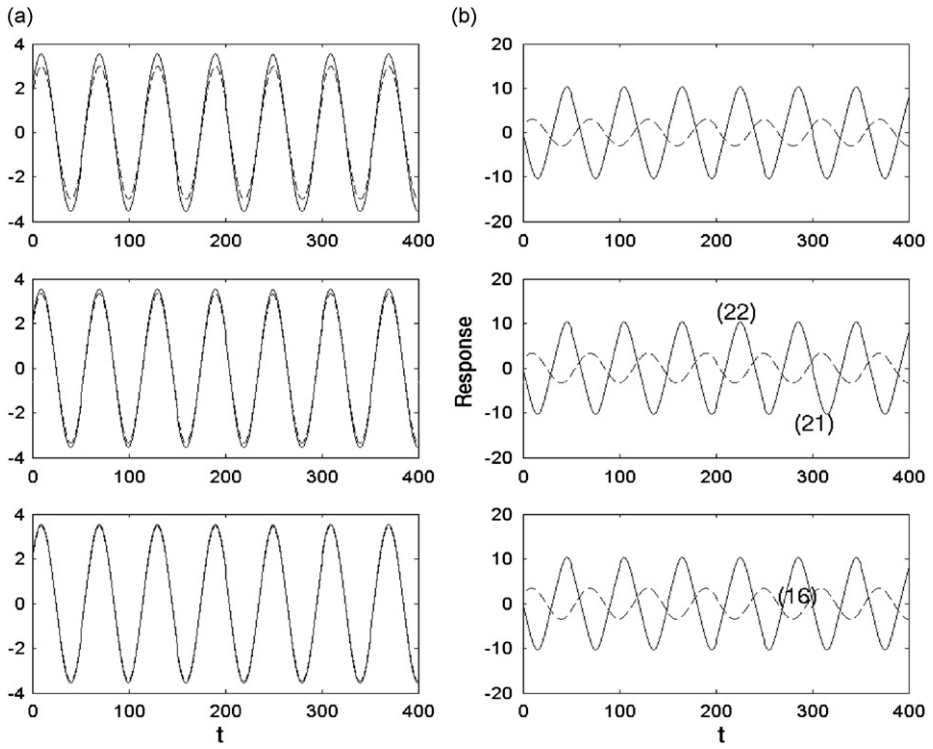

Fig. 15. Comparison of real response and synthesized response by GFRFs before and after the jump. Top—first order response, middle—up to the 3rd order response and bottom—up to the 5th order response.

A discrete time Volterra series is also called a NX (Nonlinear model with eXogenous inputs) model. Such an NX model can be built at the after-jumping point A=9.09, presented in (37). Here the excitation and response data were collected by stimulating the system (35) using fifth order Runge–Kutta method at a sampling interval $\pi/60$.

$$y(k) = 3.1948u(k-2) - 2.2584u(k-1) + 0.00882u^3(k-2) - 0.00721u^2(t-1)u(t-2) \tag{37}$$

The relevant Model Predicted output, which shows a perfect match with the real response, is given in Fig. 17. Apparently Fig. 17 suggests that the Duffing oscillator (30) at the after-jumping point A=9.09 can be very accurately modelled by the Volterra series model (36) with only up to third-order kernels.

The NX model (37) can be mapped into the frequency domain to obtain $H_1(\cdot)$ and $H_3(\cdot)$ [10]. For comparison, the first order frequency response function at the before-jumping and after-jumping points is listed in Table 2. A significant increase of $H_1(\omega)$ in magnitude is observed after the jump in order to compensate for the shock increase of the amplitude of response.

In the following section, the above analysis is extended to a more general situation over a full range of excitation frequencies.

6. Volterra modelling of the Duffing equation with varying excitation frequency

Consider again system (20) with the coefficients in (35). This time the amplitude of the excitation is kept constant at A=1. On knowing the amplitude of excitation when the jump occurs, the new criterion (16) can also be used to determine the corresponding frequency where a jump is displayed. In the current example, this frequency is calculated from (16) as ω=1.28 rad/s, which is a very good agreement with the simulation results of the resonance response curve in Fig. 18.

Clearly there is a jump in the response from point C to point D, which suggests a severe behavior change at this location. This will be studied by an inspection of (35) in the frequency domain using RSM in Fig. 19.

It can be seen that as the frequency ω increases, the GFRFs derived from Eq. (35) are valid for the range A–B (ω=0.75 rad/s) in Fig. 18. The GFRFs start to become invalid for the range B to C (ω=1.28 rad/s) in Fig. 18, and become valid again for the range D–E. In other words, in the frequency domain, besides the same jump point as in the time domain at ω=1.28 rad/s, there is another change point at around ω=0.75 rad/s. However, the change at around ω=0.75 rad/s develops gradually, and is not as abrupt as the 'jump' at ω=1.28 rad/s. This kind of frequency domain change does not appear to be revealed by traditional tools, such as the resonance diagram in Fig. 18. The response spectrum map, which is plotted in Fig. 19, does provide some information about this frequency domain change. First of all, there are no

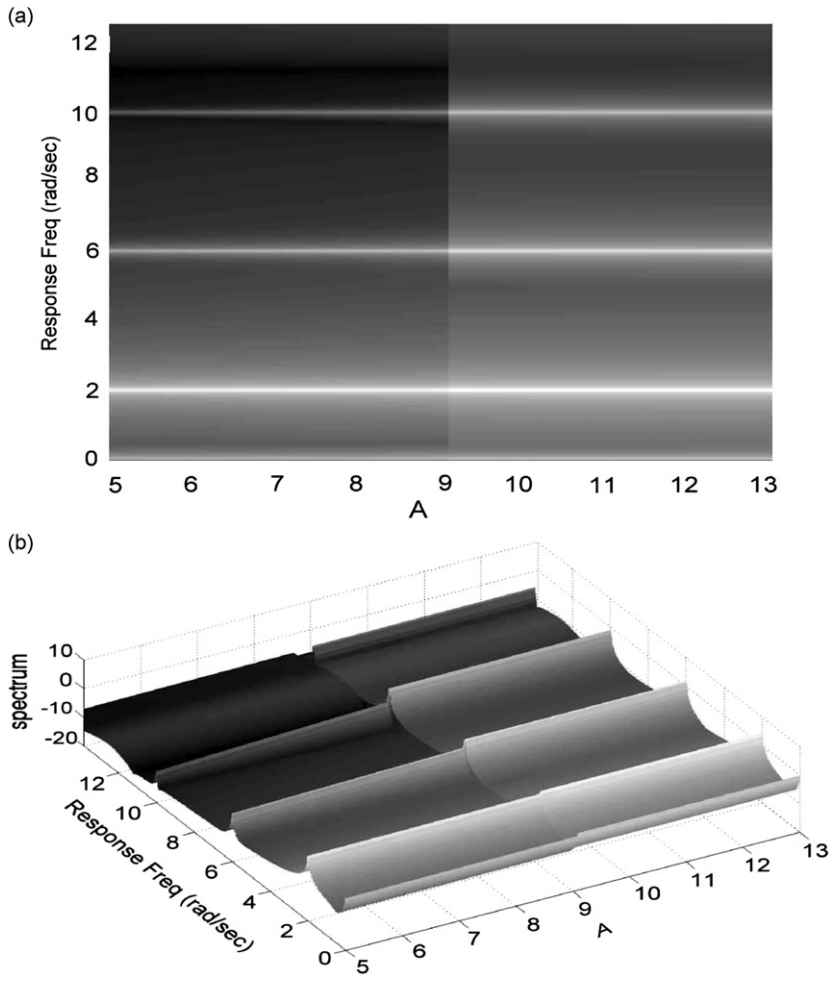

Fig. 16. RSM for system (35) when the jump occurs atω=2 rad/s: (a) 2D view and (b) 3D view.

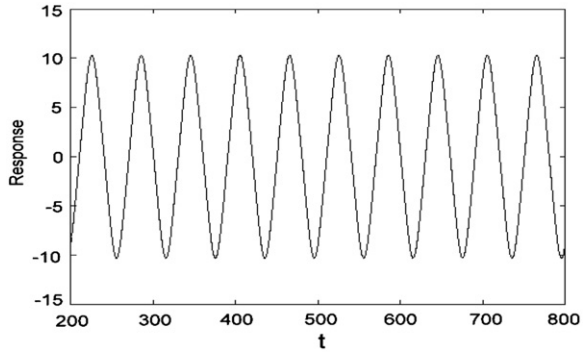

Fig. 17. Model predicted output by NX model (37): MPO—dashed and real response—solid.

Table 2
$H_1(\omega)$ before and after the jump.

$\lvert H_1(\omega)\rvert$ from (35) at A=9.08	$\lvert H_1(\omega)\rvert$ from (37) at A=9.09
0.3304	0.9777

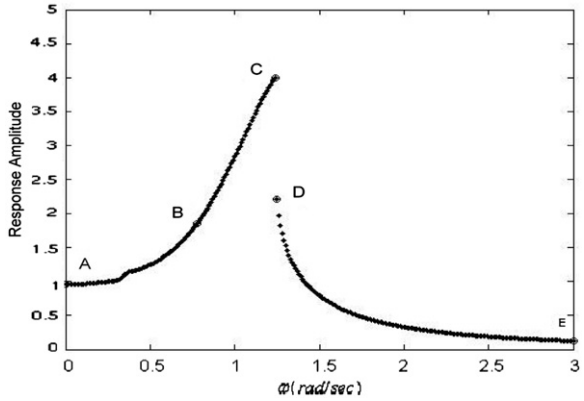

Fig. 18. Resonance response curve for Duffing equation (35) with $A=1$.

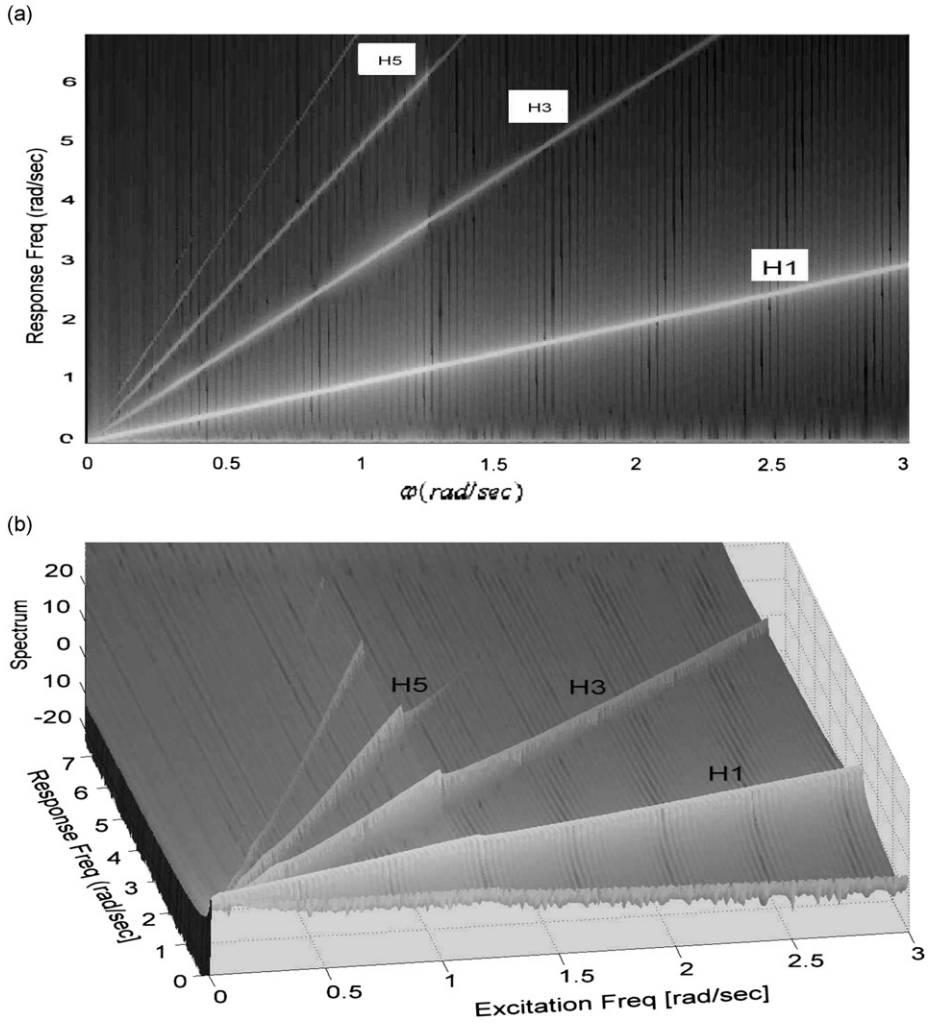

Fig. 19. Response spectrum map for Duffing equation (35) with $A=1$: (a) 2D view and (b) 3D view.

subharmonics shown in Fig. 19, suggesting that the system for the whole frequency range of interest could be mildly nonlinear and that a valid Volterra/frequency domain representation could exist over all the frequency range. Secondly, the apparent 'jump' from C to D at frequency point $\omega=1.28$ rad/s in Fig. 19 is clearly detected by the change of magnitude in

first order(linear) harmonic line H1 and the subsequent higher order harmonic lines H3, H5, etc., with a weaker harmonic presence. Fig. 19 further reveals that bigger drops are found in the higher order harmonic lines H3, H5 after the jump, with the H5 fade off very quickly. Since the higher order harmonics are associated with the higher order GFRFs, this means that before the jumping the potential Volterra series representation should have a more significant higher order kernel presence. Finally the frequency domain change at point B in Fig. 18 is not detected on the dominant first order(linear) harmonics line H1, but again the H3 line shows a significant third-order harmonic change around the frequency point ω=0.75 rad/s. In order to find the frequency domain representation for the range B–C, the technique in Section 3 can be used repeatedly, that is, discrete time Volterra—or equivalently NX—models can be identified from each pair of single tone excitation and response data, over the frequency range [0.75, 1.28]. For example, for excitation frequency ω=1 rad/s, the corresponding discrete time Volterra model can be expressed, with a sample frequency $f_s = 60/\pi$, as

$$y(k) = 26.816u(k-2) - 24.40u(k-1) + 1.3984u^3(k-2) - 1.3792u^2(k-1)u(k-2) \tag{38}$$

from which the $H_1(\cdot)$ and $H_3(\cdot)$ data at frequency ω=1 can be obtained [10].

By repeating this procedure for a number of excitation frequencies along [0.75, 1.28], the GFRFs can be acquired by putting together the frequency response data recorded at each frequency point. The first order frequency response function $H_1(\cdot)$ computed in this manner is plotted in Fig. 20 (dashed).

Using the approach introduced in [26], a nonlinear continuous time model reconstructed from the $H_1(\cdot)$ and $H_3(\cdot)$ data, is given below

$$y + 0.21727\frac{dy}{dt} + 0.87564\frac{d^2y}{dt^2} + 0.01713\frac{d^3y}{dt^3} + 0.18005\frac{d^4y}{dt^4} + 0.01939y^3 - 0.002162y^2\frac{dy}{dt} - 0.04358y\left(\frac{dy}{dt}\right)^2 + 0.0001961\left(\frac{dy}{dt}\right)^3 = u(t) \tag{39}$$

The $H_1(\cdot)$ computed from Eq. (39) [9] (solid) is compared with the $H_1(\cdot)$ from the Volterra modelling such as Eq. (38), in Fig. 20, which shows a good match.

To test the validity of the reconstructed continuous time model (39), arbitrarily choose an excitation frequency from the specific frequency range [0.75, 1.28], say, ω=0.9 rad/s, and compare the response from the original Duffing equation (35)

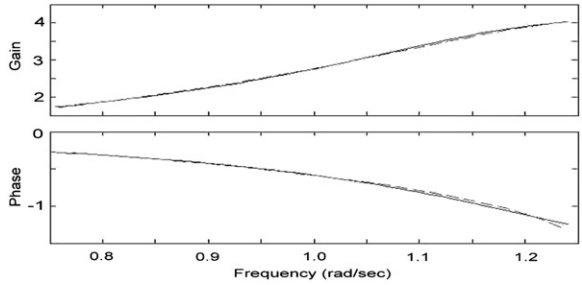

Fig. 20. $H_1(\cdot)$ by reconstructed continuous time model (39)—solid and $H_1(\cdot)$ by Volterra modelling—dashed.

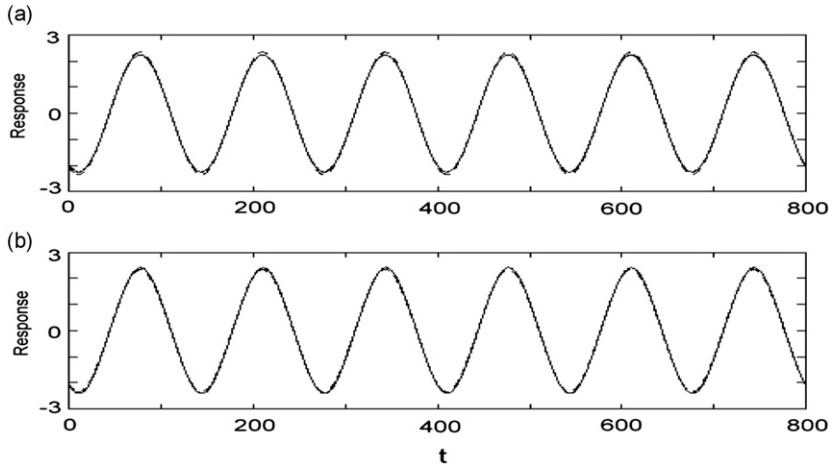

Fig. 21. (a) First order output response and (b) up to the third-order response solid—synthesized output by GFRFs from (39); dashed—simulated original output from (35).

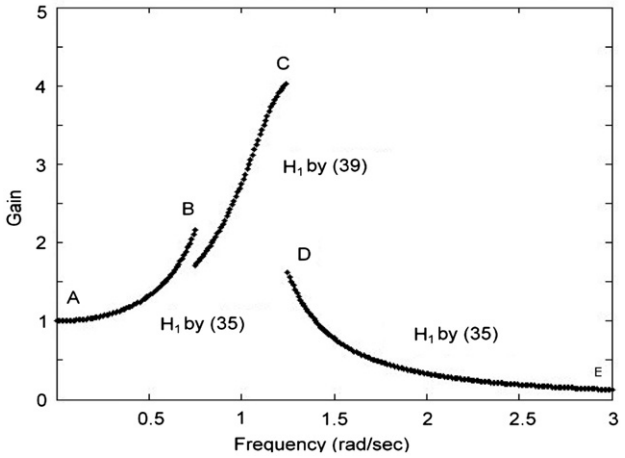

Fig. 22. First order frequency domain response function for the Duffing oscillator (35).

and the response synthesized from the GFRFs obtained from Eq. (39). It can be seen that up to third-order GFRFs from (39) can provide a satisfactory representation for the system, as shown in Fig. 21.

In summary the whole picture of the frequency domain representation for the Duffing oscillator (35) when the excitation amplitude is fixed as $A=1$ would look like Fig. 22 for the first order frequency response function for example. In summary, the frequency response function initially follows H_1 from the original Duffing equation (35) from A to B, then moves to H_1 by the new Eq. (14) from B to C, and finally jumps back to H_1 by the original Duffing equation (8) from D to E.

7. Conclusions

The Volterra series representation has been extensively studied and applied in the modelling, analysis and control of nonlinear systems. However, it has a limited convergence. It is therefore desirable to establish the convergence radius. A new criterion has been derived in this article by extending the previous time domain work to periodically excited nonlinear differential equations based on a truncated Volterra series representation. It has been shown that in many cases this new criterion can produce a more accurate estimation of the upper limit of the convergence region than the previously proposed criteria. This criterion is especially useful from the practical viewpoint for systems that require quick convergence in the Volterra domain.

The advantage of the new criterion becomes more evident when it is applied in the prediction of the upper limits of Volterra series representation for Duffing oscillators that exhibit a common type of severe nonlinearity called a shock jump in the response. The discussion in this paper shows that the jump is the dividing point between the validity of the Volterra series representation, or in other words, the absolute upper limit of a valid Volterra representation, therefore the new frequency domain criterion of this paper can be readily used in predicting the onset point of the jump, which is proved to be very successful. The scheme behind the derivation of the new criterion, that is, the nonlinear system should be efficiently described by the first few Volterra kernels, can at the same time provide some explanation of the mechanism of the formation of the jump.

A global Volterra series representation for the nonlinear oscillator involving jump phenomenon is not expected due to the analytic nature of the Volterra description. However, local Volterra series representations are still possible. This point has been discussed and analyzed using illustrative examples in this study.

Acknowledgements

The authors gratefully acknowledge that this work was supported by the Engineering and Physical Sciences Research Council (EPSRC) UK, and an European Research Council Advanced Investigator Award.

References

[1] J.F. Barrett, The use of Volterra Series to find region of stability of a non-linear differential equation, *International Journal of Control* 1 (1965) 209–216.
[2] V. Volterra, *Theory of Functionals*, Blackie and Sons, 1930.
[3] M. Schetzen, *The Volterra and Wiener Theories of Non-linear System*, Wiley, New York, 1980.
[4] W.J. Rugh, *Nonlinear System Theory—The Volterra/Wiener approach*, The John Hopkins University Press, 1981.
[5] W. Sandberg, A perspective on system theory, *IEEE Transactions on Circuits and Systems CAS* 31 (1984) 88–103.
[6] S.W. Nam, E.J. Powers, Application of higher order spectral analysis to cubically non-linear system identification, *IEEE Transactions on Signal Processing* 42 (1994) 1746–1766.

[7] S.A. Billings, K.M. Tsang, Spectral analysis for nonlinear systems, part II—interpretation of nonlinear frequency response functions, *Mechanical Systems and Signal Processing* 3 (1989) 341–359.
[8] J.J. Stoker, *Nonlinear Vibrations in Mechanical and Electrical Systems*, Inter-science Publishers, Inc., New York, 1957.
[9] S.A. Billings, J.C. Peyton Jones, Mapping non-linear integro-differential equations into the frequency domain, *International Journal of Control* 52 (1990) 863–879.
[10] J.C. Peyton Jones, S.A. Billings, A recursive algorithm for computing the frequency response of a class of non-linear difference equation models, *International Journal of Control* 50 (1989) 1925–1940.
[11] J.F. Barrett, The use of functionals in the analysis of nonlinear physical systems, *Journal of Electronics and Control* 15 (1963) 567–615.
[12] E. Bedrosian, S.O. Rice, The output properties of Volterra systems (nonlinear systems with memory) driven by harmonic and Gaussian inputs, *Proceedings of the IEEE* 59 (1971) 1688–1707.
[13] G.R. Tomlinson, G. Manson, G.M. Lee, A simple criterion for establishing an upper limit to the harmonic excitation level of the Duffing oscillator using the Volterra Series, *Journal of Sound and Vibration* 190 (1996) 751–762.
[14] A. Chatterjee, N.S. Vyas, Convergence analysis of Volterra series response of nonlinear systems subjected to harmonic excitation, *Journal of Sound and Vibration* 236 (2000) 339–358.
[15] Z.K. Peng, Z.Q. Lang, On the convergence of the Volterra-series representation of the Duffing's oscillators subjected to harmonic excitations, *Journal of Sound and Vibration* 305 (2007) 322–332.
[16] S.A. Billings, O.M. Boaghe, The response spectrum map, a frequency domain equivalent to the bifurcation diagram, *International Journal of Bifurcation and Chaos* 11 (2001) 1961–1975.
[17] C. Hayashi, *Nonlinear Oscillations in Physical Systems*, McGraw-Hill, New York, 1964.
[18] A.H. Nayfeh, D.T. Mook, *Nonlinear Oscillations*, John Wiley and Sons, New York, 1979.
[19] M.J. Feigenbaum, Universal behaviour in nonlinear systems, *Los Alamos Science* 4 (1980).
[20] D.R. Frey, O. Norman, An integral equation approach to the periodic steady-state problem in nonlinear circuits, *IEEE Transactions on Circuits and Systems I—Fundamental Theory and Applications* 39 (1992) 744–755.
[21] J.M.T. Thompson, H.B. Stewart, *Nonlinear Dynamics and Chaos*, John Wiley and Sons, New York, 1991.
[22] S.S. Rao, *Mechanical Vibrations*, Addison-Wesley, New York, 1995.
[23] Boaghe, S.A. Billings, Subharmonic oscillation modelling and MISO Volterra series, *IEEE Trans on Circuits and Systems—I: Fundamental Theory and Applications* 50 (2003) 877–884.
[24] L.M. Li, S.A. Billings, Discrete time subharmonic modelling and analysis, *International Journal of Control* 78 (2005) 1265–1284.
[25] H.J. Pain, *The Physics of Vibrations and Waves*, John Wiley & Sons, Ltd, 2005.
[26] L.M. Li, S.A. Billings, Continuous time non-linear system identification in the frequency domain, *International Journal of Control* 74 (2001) 1052–1061.